URSI GASS 2023, Sapporo, Japan, 19 – 26 August 2023

3D-Printed Smooth-Walled Conical Horn Antennas: Manufacturing and Quasioptical Analysis

Ricardo A. M. Pereira(1), Alessandra Costanzo*(2), Diego Masotti*(2), and Nuno Borges Carvalho(1)
(1) Institute of Telecommunications, University of Aveiro, Aveiro, Portugal; e-mail: r.pereira@ua.pt; nbcarvalho@ua.pt
(2) University of Bologna, Bologna, Italy; e-mail: alessandra.costanzo@unibo.it; diego.masotti@unibo.it

Abstract

Wireless power transfer systems may include focusing components to reduce spillover losses. In that case, the implementation of the theory of quasioptics assists in their optimization. This paper presents two 3D printed smooth-walled conical horn antennas used in one such system, at 5.8 GHz. This method results in a high performance, low-cost and lightweight antenna. This discussion includes the design, simulation, manufacturing and experimentation of the horns. Besides testing in an anechoic chamber for analysis of traditional antenna theory quantities, the electric field obtained through electromagnetic simulations is used to study the gaussian beam generated by the horns.

1 Introduction

With the goal of increasing the beam efficiency of radiative wireless power transfer (WPT) systems, we implemented the quasioptical framework [1], which enables us to significantly reduce the spillover losses by focusing the electromagnetic (EM) energy. This theory consists in approximating EM radiation which gaussian beams and has been used mostly in material characterization and radio astronomy, and so one can find references regarding the gaussian beams generated by horn antennas [1].

One of the WPT systems we designed with QO used a dielectric lens for focusing energy [2], while another consisted in a reciprocal double-reflector configuration [3]. Each of these used smooth-walled conical horns as transmitters and receivers, at 24 GHz and 5.8 GHz, respectively, due to how well they generate gaussian beams, while being relatively easy to manufacture. The present paper discusses the conical horn developed for the 5.8 GHz system, from initial design, simulation, manufacturing through 3D printing and copper taping, to experimentation.

Numerous antennas built through 3D printing can be found [4], [5], even for horn antennas [6], [7]. The latter reference includes two different methods for applying the metal layer, through copper tape and copper paint spray, with the former achieving a much higher conductivity, reason for which this method is the one used in the present study.

Importantly, by 3D-printing, we are referring to printing of plastic and later metalization of the structure. This term is often associated with the direct printing of metal, but it is more commonly referred to as additive manufacturing [8], and we will follow this distinction.

The main objective of this paper is to show that 3D-printing can be successfully implemented to create low-cost, lightweight and high-performance antennas, while discussing the overall parameters of such horns, from antenna theory to quasioptics.

2 Quasioptics

The formalism of quasioptics (QO) approximates EM radiation to gaussian beams. These mathematical quantities provide information about the beam radius, ϖ, and the way it varies through space, accounting for its divergence. For a beam propagating in the $\hat{z}$ direction, the minimum value of the beam radius is the beam waist, ϖ_0. This is located in z_0, and is where the power is most concentrated. The description of a gaussian beam's electric field takes this point as reference. A beam in the fundamental mode is axially symmetric, depending only on the distance to the axis of propagation (radius), r, and the point along the axis, z, where the analysis is taken:

$$E(r,z) = \sqrt{\frac{2}{\pi\varpi^2}} \exp\left(-\frac{r^2}{\varpi^2} - ikz - \frac{i\pi r^2}{\lambda R} + i\phi_0\right), \quad (1)$$

where R is the radius of curvature of the wave front, ϕ_0 is the phase shift and λ is the wavelength. Most importantly for WPT, the beam radius is defined as the radial distance at which the power density falls to $1/e$ of the on-axis value, with e being the Euler's number and is given by

$$\varpi = \varpi_0 \sqrt{1 + \left(\frac{\lambda z}{\pi \varpi_0^2}\right)^2}. \quad (2)$$

Another important quantity is the confocal distance, z_c, which details the distance from z_0 where the beam's divergence is minimal, $z_c = \pi\varpi_0^2/\lambda$.

2.1 Conical Horn Antennas in Quasioptics

As mentioned previously, horns are one of the best generators of gaussian beams, achieving one of the highest coupling efficiencies with $\eta_G = 91\%$ [1]. This value is

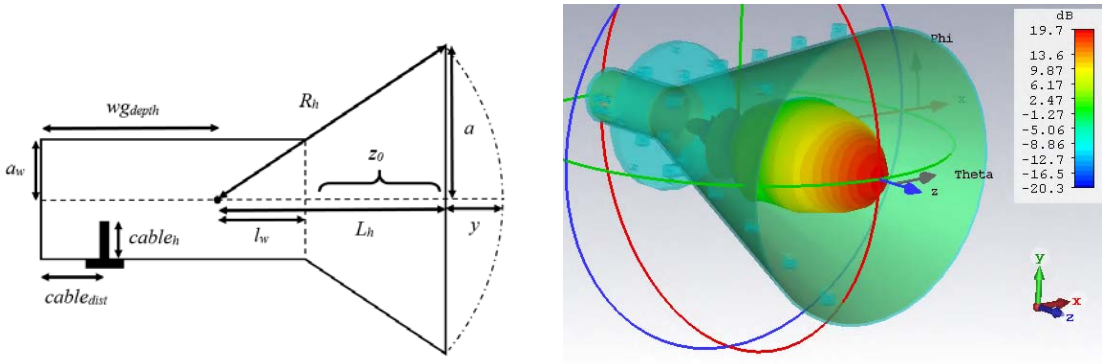

(a) (b)

Figure 1. a) Conical horn antenna schematic where a is the aperture radius, L_h is the length between the aperture and the center of curvature and R_h is the horn slant length. b) Horn far field simulation result. Both the antenna 3D printing filament and copper layers are visible.

achieved when the relationship between the antenna's aperture, a, and the gaussian beam radius at this position, ϖ_{ap}, is $\varpi_{ap} = c_g a$, with $c_g = 0.76$. The beam waist and its location are determined by assuming that the antenna's slant length, equals the beam's radius of curvature, $R = R_h$. Then, we can use the equations (3) from Ref. [1]:

$$\varpi_0 = \frac{\varpi}{\left[1 + (\pi\varpi^2/\lambda R)^2\right]^{0.5}} \quad \text{and} \quad z_0 = \frac{R}{1 + (\lambda R/\pi\varpi^2)^2}. \tag{3}$$

3 Design and Simulation

When designing the WPT system, the initial step was understanding how the beam generated by the horn would be transformed by the reflectors. An in-depth discussion can be found in Refs. [3], [9]. The required beam waist was decided to be $\varpi_0 = 4.902\,\text{cm}$, which is located inside the horn at $z_0 = 8.719\,\text{cm}$ from the aperture. Then, a horn antenna was designed following the steps detailed in [10], whose dimensions are described in Table 1 and visible in Fig. 1a. As discussed previously, the horn's aperture and slant length are related to the beam radius. Regarding the waveguide, choosing a radius of 2 cm leads to a cutoff frequency of 4.395 GHz for the TE_{11} propagation mode, which was excited through a SMA connector.

After arriving at the intended dimensions, the horn was designed and simulated in the *CST Studio Suite* software. An optimization of the antennas' dimensions was performed to arrive at the best device possible. Both the 3D-printed filament of polylactic acid (PLA) layer and the conductive copper layer were included in the simulation (Fig. 1b).

The antenna's simulated return loss and gain at 5.8 GHz are $-30.6\,\text{dB}$ and 19.6 dBi, respectively, while the antenna's total efficiency is 98%. Additionally, the horn's electric field was extracted for obtaining the gaussian beam parameters.

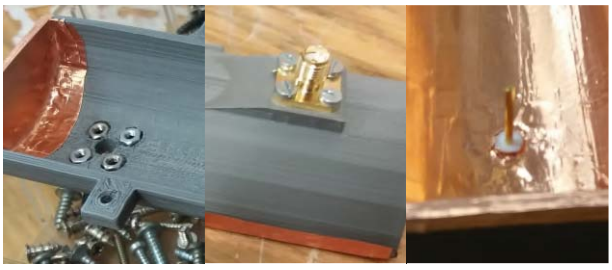

(a) (b) (c)

Figure 2. The 3D printed horn antenna at different stages of the copper taping. a) Placement of the connector's nuts. b) Fixation of the connector. c) Covering of the copper around the connector.

These will be discussed in section 5. The antenna results are summarized in Table 2.

4 Manufacturing and Experimentation

The optimized design of the antenna was used for the 3D-printing. But since the antenna was larger than the available space of the printer, the design was divided into four pieces. Hence, supports were included in the design for later enabling their fixation into a single unit through bolts and nuts. This final design is the one that was simulated and is visible in Fig. 1b. Two antennas were printed, for transmission and reception. The printed pieces were sanded and the support holes widened. Then, the copper tape was applied to all the pieces individually and, after they had been strapped together, to the intersections between the pieces.

Noteworthily, the connectors were fixed by bolts and nuts, whose positioning was included in the 3D printed pieces. Due to this fixation mechanism, the connectors were installed before finishing the copper tape, as can be seen in Fig. 2a and 2b. After guaranteeing electrical contact from the connector ground to the horn's surface, the bolts were

Table 1. Conical horn antenna design parameters.

Symbol	Terminology	Value [cm]
a	Aperture Radius	10.893
R_h	Slant Length	30.587
L_h	Horn Length	28.582
l_w	Waveguide Length	5.224
ϖ_0	Beam Waist	4.902
z_0	Beam Waist Location	8.719

Table 2. Gain [dBi] and measured return loss [dB] of the antennas.

Symbol	Terminology	Value [dBi] and [dB] Ant. 1	Ant. 2
G_{design}	Intended Gain value	19.000	
G_{sim}	Gain from simulation	19.600	
G_{meas}	Measured Gain	19.064	19.064
S_{11}	Measured Return Loss	-30.934	-18.357

cut to fit in the spacing and the remaining copper was taped (Fig. 2c). Afterwards, the connector length was cut into the optimal size. Two different bolt and nut sets were used, one made of metal and the other of plastic. While initially expecting the plastic ones to be better due to a reduced electromagnetic interference, experimental testing showed very identical results. Additionally, the plastic set ended breaking up while using a torque wrench for connecting the SMA connector to a SMA cable, prompting the use of metal sets in the future.

On the other hand, the fast cooling of the PLA filament when printing into the support glass led to warping of some of the pieces. This deformation did not significantly affect the shape, and therefore performance, of the antennas. This is because when the pieces were put together, the fixation strength forced the deformed pieces into place, even leading to some cracks in the plastic.

After their manufacturing, a copper antioxidant spray was applied. Then, both the antennas were tested in an anechoic chamber. With this purpose in mind, a disk as built into the antenna's design, enabling an easy connection to the anechoic chamber's support, as visible in Fig. 3a.

5 Quasioptical Analysis

The electric field obtained from the EM simulation was used for analyzing the parameters of the gaussian beam generated by the horns. This was achieved by analyzing the field distribution in the XZ and YZ planes. At each point in space, the value of the field on the axis of propagation, $\hat{z}$, was obtained and used to determine the radius where the field fell by $1/e$. Naturally, for each z there are two values, up and below the axis, which are visible in Fig. 4. The used beam radius was an average of both of these values.

Table 3. Gaussian beam parameter obtained from the fitting algorithm.

Symbol	Terminology	Value [cm] XZ	YZ
ϖ_0	Fitted beam waist	4.751	7.008
z_0	Fitted waist location	13.302	2.432

Then, points considered inadequate were excluded from the fitting. These were either inside the horn or too close to it, where the near field effects were deemed significant. On the other hand, points at the edges of the simulated space were also excluded. This resulted in using the points where 65 cm $< z <$ 124 cm. For reference, the horn aperture is located at 31 cm and the simulation space ends at 134 cm.

The curve fitting was performed via the method of nonlinear least squares, allowing the determination of the beam waist and its location, which best fit the data. This is done by using (2) and adjusting z to be the z coordinate of each point and including z_0 for the waist location. The equation to fit is then $\varpi = \varpi_0 \left[1 + [(\lambda (z - z_0))/(\pi \varpi_0^2)]^2\right]^{1/2}$. In this fitting, ϖ corresponds to the dependent variable, while z is the independent one, while z_0 and ϖ_0 are the parameters to be fitted. The constants were defined as a single fixed parameter, $m = \lambda/\pi$.

The beam parameters that best fit the data are different for each plane, as was expected for the smooth-walled conical horns, due to the differences caused by the feeding of the waveguide mode. The obtained parameters fit the data with a high value of R^2, although the results in the XZ plane are much closer to the theoretical one (Table 3).

6 Conclusions

Two smooth-walled conical horn antenna at 5.8 GHz, which were designed taking into account quasioptical requirements.

Simulations were performed for validation and optimization, which enabled the extraction of gaussian beam parameters in two planes in an novel way. After simulation, a method for manufacturing a smooth-walled conical horn antenna was presented using 3D-printing. The built antennas were tested in an anechoic chamber, revealing high-performance for a relatively low cost and lightweight solution. An important conclusion is that for fixing the SMA connector, it is recommended to use metallic bolts and nuts instead of plastic.

Future work includes simulating the antenna with a higher resolution mesh, repeat the analysis while allowing for asymmetrical beams. Additionally, the electric field distribution in the XY plane will be used for calculating the gaussian coupling efficiency. Nevertheless, a method for manufacturing a conical horn antenna and analyzing the

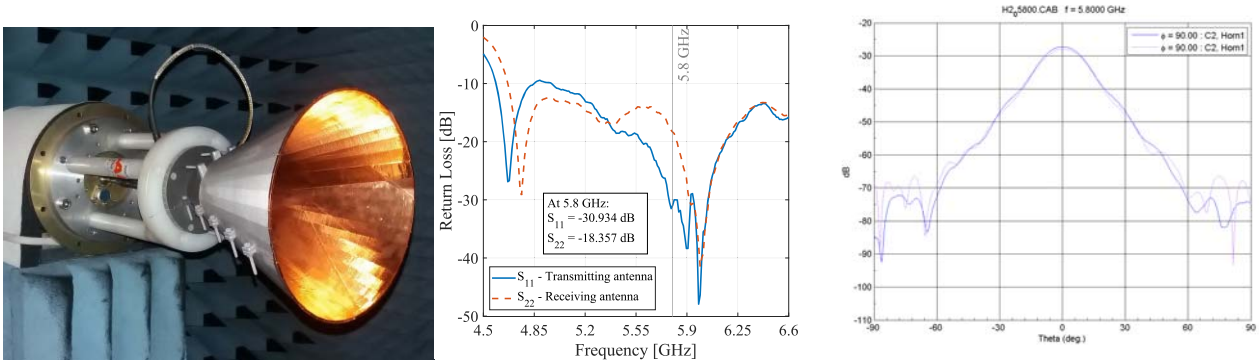

(a) (b) (c)

Figure 3. a) Final 3D-printed horn antenna. b) Both horn antennas' return losses. c) Both horn antennas' gain.

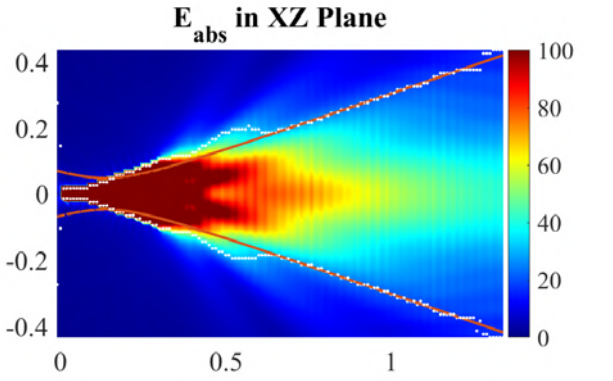

Figure 4. Electric field distribution, where the beam waist points are marked by white dots, and the fitted gaussian beam is shown in orange.

gaussian beam it produces has been presented here, with high-performance radiation characteristics.

Acknowledgements

The authors would like to acknowledge the contributions of Hugo Mostardinha and Paulo Gonçalves who assisted in the manufacture of the antennas.

Ricardo A. M. Pereira would like to thank the Fundação para a Ciência e a Tecnologia (FCT), Portugal, for his Ph.D. grant SFRH/BD/145024/2019, as well as the European Microwave Association for the Internship Award 2022.

This work is also funded by FCT/MCTES through national funds and when applicable co-funded EU funds under the project UIDB/50008/2020-UIDP/50008/2020.

References

[1] P. F. Goldsmith, *Quasioptical Systems: Gaussian Beam Quasioptical Propagation and Applications*. Piscataway, NJ, IEEE Press, 1998.

[2] R. A. M. Pereira and N. B. Carvalho, "Quasioptical dielectric lens system for WPT solutions," in *2022 Wireless Power Week (WPW)*, 2022, pp. 190–194. doi: 10.1109/WPW54272.2022.9853933.

[3] R. A. M. Pereira and N. B. Carvalho, "Quasioptics for increasing the beam efficiency of wireless power transfer systems," *Sci. Rep.*, **12**, 1, p. 20 894, 2022. doi: 10.1038/s41598-022-25251-w.

[4] M. I. M. Ghazali *et al.*, "Affordable 3d printed microwave antennas," in *2015 IEEE 65th Electr. Comp. and Tech. Conf. (ECTC)*, 2015, pp. 240–246. doi: 10.1109/ECTC.2015.7159599.

[5] J. Bjorgaard *et al.*, "Design and fabrication of antennas using 3d printing," *Progr. In Electrom. Res. C*, **84**, pp. 119–134, 2018.

[6] H. Yao *et al.*, "Ka band 3d printed horn antennas," in *2017 Texas Symp. on Wirel. and Microwave Circ. and Sys. (WMCS)*, 2017, pp. 1–4. doi: 10.1109/WMCaS.2017.8070701.

[7] J. Teniente *et al.*, "3-d printed horn antennas and components performance for space and telecommunications," *IEEE Antennas Wirel. Propag. Lett.*, **17**, 11, pp. 2070–2074, 2018. doi: 10.1109/LAWP.2018.2870098.

[8] S. A. Tofail *et al.*, "Additive manufacturing: Scientific and technological challenges, market uptake and opportunities," *Mater. Today*, **21**, 1, pp. 22–37, 2018, ISSN: 1369-7021. doi: https://doi.org/10.1016/j.mattod.2017.07.001.

[9] R. A. M. Pereira, N. B. Carvalho, and A. Georgiadis, "Focus location measurement of a quasioptical double reflector system," in *2021 IEEE Wirel. Power Transfer Conf. (WPTC)*, 2021, pp. 1–4. doi: 10.1109/WPTC51349.2021.9457870.

[10] Y. T. Lo and S. W. Lee, *Antenna Handbook: Volume II Antenna Theory*. New York, NY: Van Nostrand Reinhold, 1993.